



**HAL**  
open science

## Reliability of B-mode ultrasound and shear wave elastography in evaluating sacral bone and soft tissue characteristics in young adults with clinical feasibility in elderly

Maher Abou Karam, Ekaterina Mukhina, Nils Daras, Isabelle Rivals, Helene Pillet, Wafa Skalli, Nathanael Connesson, Yohan Payan, Pierre-Yves Rohan

### ► To cite this version:

Maher Abou Karam, Ekaterina Mukhina, Nils Daras, Isabelle Rivals, Helene Pillet, et al.. Reliability of B-mode ultrasound and shear wave elastography in evaluating sacral bone and soft tissue characteristics in young adults with clinical feasibility in elderly. *Journal of Tissue Viability*, 2022, 10.1016/j.jtv.2022.02.003 . hal-03584731

**HAL Id: hal-03584731**

**<https://hal.science/hal-03584731v1>**

Submitted on 22 Feb 2022

**HAL** is a multi-disciplinary open access archive for the deposit and dissemination of scientific research documents, whether they are published or not. The documents may come from teaching and research institutions in France or abroad, or from public or private research centers.

L'archive ouverte pluridisciplinaire **HAL**, est destinée au dépôt et à la diffusion de documents scientifiques de niveau recherche, publiés ou non, émanant des établissements d'enseignement et de recherche français ou étrangers, des laboratoires publics ou privés.

1 **Reliability of B-mode Ultrasound and shear wave**  
2 **elastography in evaluating sacral bone and soft tissue**  
3 **characteristics in young adults with clinical feasibility**  
4 **in elderly**

5 **Maher Abou Karam<sup>a</sup>, Ekaterina Mukhina<sup>b</sup>, Nils Daras<sup>a</sup>, Isabelle Rivals<sup>c,d</sup>,**  
6 **Helene Pillet<sup>a</sup>, Wafa Skalli<sup>a</sup>, Nathanaël Connesson<sup>b</sup>, Yohan Payan<sup>b</sup>, Pierre-Yves**  
7 **Rohan<sup>a,\*</sup>**

8 <sup>a</sup> *Institut de Biomécanique Humaine Georges Charpak, Arts et Métiers ParisTech, 151 bd de l'Hôpital, 75013 Paris, France*

9 <sup>b</sup> *Univ. Grenoble Alpes, CNRS, Grenoble INP, TIMC-IMAG, Grenoble, France*

10 <sup>c</sup> *Sorbonne Université, INSERM, UMRS1158 Neurophysiologie Respiratoire Expérimentale et Clinique, Paris, France*

11 <sup>d</sup> *Equipe de Statistique Appliquée, ESPCI Paris, PSL Research University, Paris, France*

12

13 **Keywords:** pressure ulcer, sacrum, medial sacral crest, elderly, ultrasound, shear wave elastography, elasticity,  
14 **reliability**

15 *List of abbreviations:*

16 B-mode, Brightness mode; CI, confidence interval; CT, Computed tomography; FE, Finite element; HT, Hypodermis  
17 thickness; hSWE, hypodermis shear wave elastography; HE, Medial sacral crest height; ICC, intraclass correlation  
18 coefficient; IT, ischial tuberosity; MRI, Magnetic resonance imaging; MSC, Medial sacral crest; mSWE, muscle shear  
19 wave elastography; OA, Medial sacral crest opening angle; PSIS, Posterior superior iliac spine; PU, Pressure ulcer;  
20 ROC, Medial sacral crest radius of curvature; ST, Skin thickness; SWE, Shear wave elastography; sSWE, Skin shear  
21 wave elastography; US, ultrasound.

22

23

## 24 **Highlights**

- 25 • In the elderly loss of mobility, sarcopenia, skin atrophy, and loss of elasticity contribute to the occurrence of a  
26 pressure ulcer (PU)
- 27 • Bedside B-mode US and SWE protocol was proposed to evaluate skin, hypodermis, and muscle morphology  
28 and mechanical properties
- 29 • The protocol was tested for reliability on 19 healthy young subjects, and clinical feasibility on 11 healthy older  
30 people
- 31 • Reliability was mostly unsatisfactory despite efforts to standardize protocol and measurement definitions
- 32 • Perspective work will review protocol to increase reliability and evaluate risk in elderly in nursing homes

## 33 **Abstract**

34 *Background:* Physiologic aging is associated with loss of mobility, sarcopenia, skin atrophy and loss of elasticity.  
35 These factors contribute, in the elderly, to the occurrence of a **pressure ulcer (PU)**. Brightness mode ultrasound (US)  
36 and **shear wave elastography (SWE)** have been proposed as a patient-specific, bedside, and predictive tool for PU.  
37 However, reliability and clinical feasibility in application to the sacral region have not been clearly established.

38 *Method:* The current study aimed to propose a simple bedside protocol combining US and SWE. The protocol was  
39 first tested on a group of 19 healthy young subjects by two operators. The measurements were repeated three times.  
40 Eight parameters were evaluated at the medial sacral crest. Intraclass Correlation Coefficient (ICC) was used for  
41 reliability assessment and the modified Bland Altman plot analysis for agreement assessment. The protocol was then  
42 evaluated for clinical feasibility on a healthy older group of 11 subjects with a mean age of  $65 \pm 2.4$  yrs.

43 *Findings:* ICC showed poor to good reliability except for skin SWE and hypodermis thickness with an ICC (reported  
44 as: mean(95%CI)) of 0.78(0.50-0.91) and 0.98(0.95-0.99) respectively. No significant differences were observed

45 between the young and older group except for the muscle Shear Wave Speed (SWS) (respectively  $2.11 \pm 0.27$  m/s vs  
46  $1.70 \pm 0.17$  m/s).

47 *Interpretation:* This is the first protocol combining US and SWE that can be proposed on a large scale in nursing  
48 homes. Reliability, however, was unsatisfactory for most parameters despite efforts to standardize the protocol and  
49 measurement definitions. Further studies are needed to improve reliability.

50

## 51 **Introduction**

52 Tissue morphology, mechanical properties, physiology, and repair properties can all change over time as a result of  
53 aging, lifestyle, chronic injury, or disease. Over a bony prominence, these changes - associated with a mechanical load  
54 - can lead to a localized injury known as a “pressure ulcer” [1].

55 The prevalence of this lesion ranges between 9% [2] and 15% [3] in long term care or hospitalized patients , and is  
56 most frequently observed over the sacrum or the heel. Two thirds of PU are observed in patients above 70 years of age  
57 [4]. The occurrence of PU is associated with significant increase in hospital costs, length of stay and, most importantly,  
58 an increased risk of death. [5]–[7].

59 While numerous and efficient therapies have been developed, prevention remains the center of interest of all healthcare  
60 professionals and thus of researchers [4]. However, current practices in PU prevention are far from satisfactory with  
61 more than 85% lack in documented repositioning care plan. This is majorly due to the lack of staff and time [2]. PU  
62 prevention protocols are based on risk assessment tools or scales (Norton scale, Braden scale...) [8]. The impact of  
63 these tools on the incidence of PU remains uncertain and fail to meet the needs of all patients in different clinical  
64 settings [7].

65

66 The process of aging is associated with physiological changes including sarcopenia, osteoporosis, progressive increase  
67 in blood glucose and skin atrophy [9]. The decrease in muscular power has a high impact on the performance of daily  
68 activities even in healthy older persons leading to increased immobility [10]. In consequence, the elderly are  
69 considered at risk of developing PU and therefore, a target group for preventive screening protocols. Several bedside  
70 technologies combined with assessment tools were investigated for early detection of PU, especially in long term care

71 facilities. High frequency ultrasound (HFUS) was particularly studied, given its accessibility and capacity to detect  
72 preclinical superficial skin changes, mainly the presence of fluid/oedema at different levels of the skin [11]. However,  
73 a randomized controlled trial [12] failed to demonstrate that HFUS was an effective strategy for predicting the  
74 development of Category/Stage I PUs of the heel or sacrum compared with a focused physical assessment. Also, a  
75 systematic review [13] evaluated HFUS among other technologies. Despite giving meaningful and consistent results,  
76 it could not be recommended due to lack of reliability of protocols, being limited to detecting macroscopic level tissue  
77 damage, and its training requirements for image interpretation.

78 In terms of etiology/pathophysiology, studies based on both *in vitro* (cell models) and *in vivo* (animal models)  
79 approaches have demonstrated that at least two damage mechanisms, are involved in the development of PU: first,  
80 compression damage due to tissue ischemia/reperfusion initiated by local, moderate and persistent mechanical loads;  
81 secondly, direct deformation damage above a threshold level related to shear strain; even for a short period of time  
82 (during transfer from bed to a wheelchair for example) [14]. These results suggest the presence of a direct link between  
83 mechanical determinants and biological processes leading to tissue damaging and, in fine, necrosis.

84 Based on the rationale that elucidating the relationship between external loads and internal local stresses and strains  
85 within loaded soft tissues has the potential of improving the management and prevention of PUs, several Finite  
86 Element (FE) models of the buttocks have been proposed in the literature. Models are mostly based on the  
87 segmentation of MRI or CT scan sequences [15]–[18]. However, the use of MRI and CT scans is limited due to cost,  
88 accessibility, and time [19]. In this perspective, brightness mode (B-mode) ultrasound (US) imaging was proposed as  
89 an alternative to MRI or CT-scan. Feasibility, reproducibility, and its use for personalized FE models were investigated  
90 mainly over the ischial tuberosity [19]–[23].

91 Recent studies [19], [24], [25] proposed B-mode US for the evaluation of biomechanical risk of PU in a seated position  
92 by assessing, among other parameters, tissue thickness changes in different positions. On the other hand, ultrasound  
93 elastography, a relatively new method that shows structural changes in tissues following application of physical stress  
94 can be used in the examinations of musculoskeletal system [26]. Shear wave elastography (SWE) uses focused  
95 ultrasonic beams, to remotely generate mechanical vibration sources radiating low-frequency, shear waves inside  
96 tissues [27]. It allows a bedside evaluation of the local mechanical properties of soft biological tissues by assessing  
97 shear modulus [28]–[30]. Experiments demonstrated that ultrasound elastography is a promising technique for PU  
98 detection, especially at an early stage of the pathology, when the disease is still visually undetectable [28].

99 Previous studies investigating the combination of B-mode US and SWE elastography in the context of PU prevention  
100 focused on potential changes of tissue stiffness during prolonged loading [31] or tissue characteristics in different body  
101 postures [32].

102  
103 The current study aimed to propose and test a bedside B-mode US and SWE protocol that can be used as a risk  
104 assessment tool for sacral PU in elderly. The protocol was designed for the evaluation of bone geometry, tissue  
105 morphology and mechanical characteristics over the sacrum. Reliability and reproducibility of our protocol were tested  
106 on a healthy young adults group. The protocol was then applied on a group of healthy older people to assess for clinical  
107 feasibility.

108

## 109 **Materials and methods**

### 110 **1. Data Collection**

111 The current study was approved by the ethics committee (Comité de protection des Personnes CPP NX06036) and  
112 each subject gave an informed consent. For the reproducibility analysis 19 young healthy subjects participated to the  
113 experiment, 8 women and 11 men (Age:  $25.7 \pm 3.8$  yrs, Weight:  $75.2 \pm 16.4$  kg, **BMI:  $24.5 \pm 4.9$  kg/m<sup>2</sup>**). For the  
114 elderly group 11 healthy subjects, 7 women and 4 men were recruited (Age:  $65 \pm 2.4$  yrs, Weight:  $72.5 \pm 18.6$  kg,  
115 **BMI:  $25.34 \pm 5$  kg/m<sup>2</sup>**). Exclusion criteria included: the presence of chronic or acute low back pain, history of lower  
116 spine surgery or sacral PU, and the presence of PU skin signs at the moment of the acquisition.

117

#### 118 *Ultrasound acquisition protocol*

119 B-mode US images and shear wave elastography (SWE) videos were obtained using a commercial device  
120 (SupersonicMach30, SuperSonic Imagine, France). Two probes were used, the curvilinear (SuperCurved C6-1X) with  
121 low frequency (1 to 6 MHz allowing increased depth visualization) and large field of view, and the linear (SuperLinear  
122 L10-2) probe with a higher frequency (2 to 10 MHz allowing superficial layers visualization). The general mode and  
123 penetration optimization were chosen for all acquisitions.

124 A standardized - tissue and musculoskeletal US/SWE over the sacral region - protocol was developed and was first  
125 pilot tested on a sample of three healthy young volunteers, consequently, adjustments were made. The definitive  
126 protocol is described thoroughly in Appendix 1.

127 Acquisitions were taken in the lying prone position. After anatomic palpation of the two posterior superior iliac spines  
128 (PSIS), the curvilinear probe was first used in B-mode to recognize the anatomic region of interest: the MSC. An  
129 image was captured to assess bone anatomy and the skin was marked with a tape. Switching to the linear probe, the  
130 second image captured the skin and hypodermis at the level of the MSC. The third part, also using the linear probe at  
131 the marked skin level, was a series of three videos (of 10 seconds each) in SWE mode with a region of interest (ROI)  
132 including both skin and hypodermis. For the fourth and last part, three SWE videos of the gluteus maximus muscle  
133 were taken lateral to the sacro-coccygeal region at the lower part of the sacrum. The images/videos using the linear  
134 probe were taken with minimal applied pressure, using a thick gel layer and making sure it was visible on the US  
135 image. A summary of the acquisition protocol and images are shown in figure 1.

136

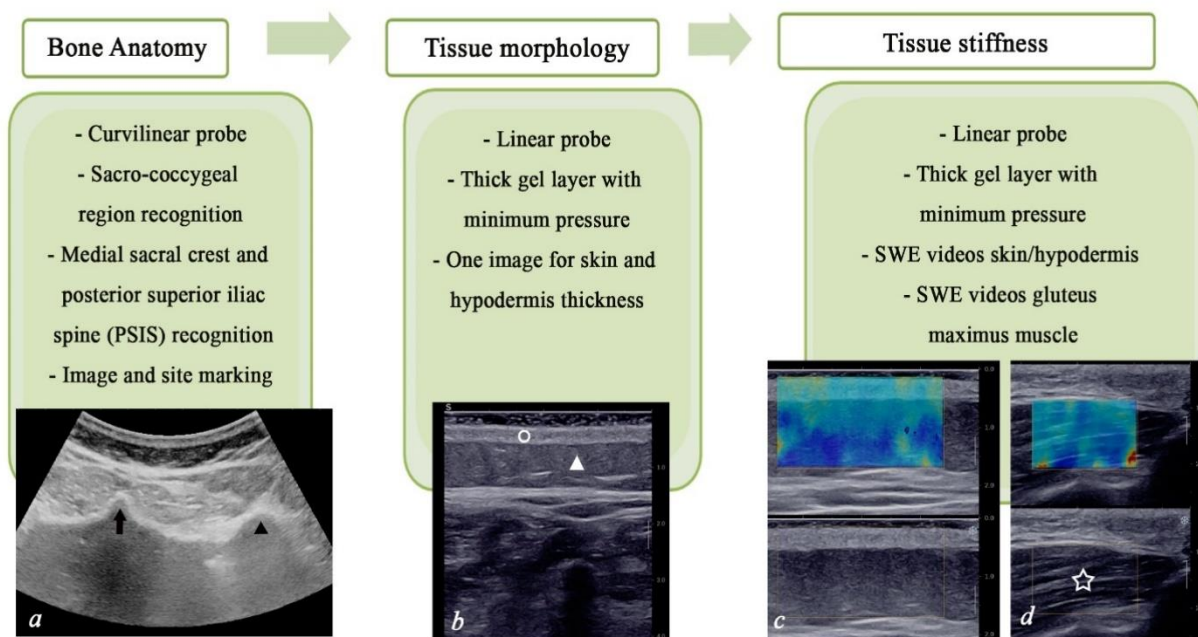


Fig. 1. US acquisition protocol of the sacral region in the transverse view. In B-mode: the medial sacral crest (arrow) at the level of the PSIS (black triangle) (a), skin (circle) and adipose tissue (white triangle) over MSC (b); in SWE mode: the skin and adipose tissue (c), gluteus maximus muscle (star) (d).

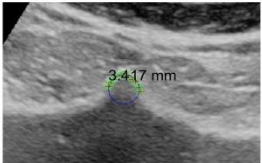
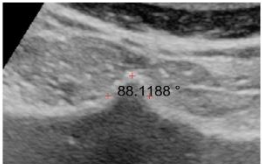
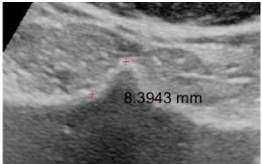
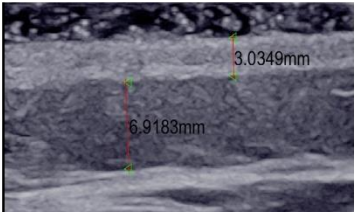
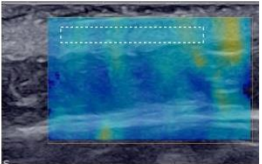
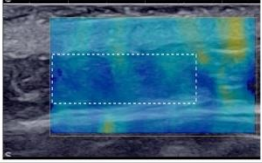
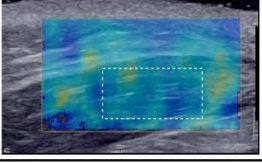
### 137 Parameter estimation

138 To reduce acquisition time, processing and measurements for images/videos were done separately using a custom

139 software written in Matlab (R2019a) (MathWorks, Inc, Natick MA). In total 8 parameters were measured using the  
140 images/videos captured during each acquisition. First, the bone anatomy image (fig.1a) was used to measure the MSC  
141 radius of curvature (ROC), opening angle (OA), and height (HE). Then, the second image (fig.1b) was used to measure  
142 the skin thickness (ST) and the hypodermis thickness (HT). For the SWE videos of the third (fig.1c) and fourth (fig.1d)  
143 part of the acquisition, images were extracted and processed using a separate written code [33]. The average value of  
144 the images of each video was calculated and then, the average of the three videos determined the shear wave velocity  
145 of one acquisition for: the skin (sSWE), the hypodermis (hSWE), and gluteus maximus muscle (mSWE). Details about  
146 the definitions and recommendations for these measurements are reported in table 1.



Table 1. Description of parameter measurement post acquisition using a customized MATLAB algorithm

	Parameter name	Description	Post-processing
<i>Bone anatomy (curvilinear probe - B-mode)</i>	Radius of curvature (ROC)	10 points distributed equally on both sides of the tip of MSC ; the circle plotted was viewed to ensure it captures the shape of the tip (19)	
	Opening angle (OA)	3 points: one on the middle of the MSC tip and two bilateral points	
	Height (HE)	3 points: the geometry of the MSC could be compared to a triangle, the tip is the highest point of the triangle and two points for the base of the MSC; the distance from the upper point to the base is the HE	
<i>Tissue morphology (linear probe - B-mode)</i>	Skin thickness (ST)	2 points: the upper limit marked by the most superficial, homogenous, and continuous line of the epidermis; lower border marked by the transition between dermis and hypochoic adipose tissue	
	Hypodermis thickness (HT)	2 points: thickest hypochoic region under the skin; hyperechoic muscle fascia marks the lower border	
<i>Tissue stiffness (linear probe - SWE mode)</i>	SWE hypodermis (hSWE)	Region of interest (ROI): largest, most homogenous SWE signal	
	SWE skin (sSWE)		
	SWE gluteus muscle (mSWE)		

148           **2.       Method Evaluation**

149       *Sample size and Reliability assessment*

150       All the data were analyzed with the IBM SPSS for Windows (Version 27.0. Armonk, NY: IBM Corp).

151       The reliability study was conducted on the young, healthy group by two operators: a physician and an engineer. Both  
152       operators received extensive training consisting of two phases: first, measurements were repeated until reaching  
153       adequate reproducibility compared with an expert sonographer then, deviations were assessed, and possible problems  
154       were determined and corrected.

155       The operators were asked to repeat the protocol three times on each subject, i.e., captured three images for each of the  
156       bone geometry parameters and tissue morphology, and nine SWE videos for each tissue stiffness parameter.

157       The reliability of our protocol was assessed by calculating the intra class correlation coefficient (ICC) for within-  
158       operator and between-operator for the young subjects group [34]. The minimum sample size required for this test-  
159       retest reliability study was estimated based on the recommendations made in Bujang et al [35]. With three observations  
160       per subject, a minimum sample size of 15 is required to detect an ICC value of 0.5 with power of 90% when taking a  
161       type I error risk of 5% (table 1a of [35]).

162       Given that ultrasound acquisition is highly operator dependent, and that the processing/measurement of a given  
163       image/video (i.e. definitions of parameters) might also differ from one operator to another, we decided to quantify the  
164       variability first at processing level, and then at both processing and acquisition level. First, the two operators processed  
165       and measured one acquisition conducted by the physician on all subjects. Each operator repeated measurement of the  
166       same image/video three times, allowing an intra-image analysis [36]. For this analysis, the ICC model 3 (2-way mixed)  
167       was chosen for within-operator reliability, and ICC model 2 (2-way random) for between-operator reliability with  
168       absolute agreement type and single measure [37]. For between operator reliability, values of one of the three  
169       measurement, chosen randomly for each operator, was used. Then, each operator processed and measured their own  
170       acquisitions allowing an inter-image analysis [36]. The same model and type for within-operator ICC (2-way mixed  
171       and absolute agreement) were used with single measure, and for between-operator reliability also the ICC model 2  
172       was used but with consistency agreement type and single measure since different images are compared. Also, for  
173       between operator reliability, values of one of the three measurements, chosen randomly for each operator, was used.  
174       This procedure was conducted for each parameter and the ICC with 95% confidence interval was reported. Values  
175       less than 0.5, between 0.5 and 0.75, between 0.75 and 0.9, and greater than 0.90 indicated poor, moderate, good, and

176 excellent reliability, respectively [37].

### 177 *Agreement assessment*

178 The modified Bland Altman plot analysis for continuous measures [38] was used as a measure of the level of agreement  
179 within and between operators for both the intra-image and inter-image analysis. **In the absence of a gold standard, the**  
180 **value of each measurement was compared to the average of all measurements for one subject (bias line equal to zero).**  
181 The difference between each observer and the overall mean for a subject is estimated. The 95% level of agreement  
182 with the mean is estimated as  $\pm 2 \times$  Standard deviation (SD), where SD represents the square root of the variance of  
183 the differences.

### 184 *Healthy young adults vs healthy elderly*

185 The same protocol was conducted once (one acquisition and measured once) on the older group by one operator: the  
186 physician. For the young adults group data, the measurements of one of the three acquisitions collected by the  
187 physician were chosen randomly. **Normality was checked with the Shapiro–Wilk test and the equality of variance was**  
188 **assessed with the Levene's test. If both normal distribution and equality of variance of the different groups could be**  
189 **assumed, data were reported per parameter and per group as mean  $\pm 1$  SD and groups (young versus old) were**  
190 **compared using the student t-test. In case the normality or equality of variance assumption was violated, groups were**  
191 **compared with the Wilcoxon test. For all the tests, the significance level was set at 0.05 *a priori*.**

## 192 **Results**

### 193 *Reliability assessment*

194 Within operator and between operator ICC with the 95% confidence interval, for both the intra and inter-image analysis  
195 for all parameters, are reported in table 2. First in the intra-image analysis, all ICC confidence interval values showed  
196 good to excellent reliability for within operator, except for the ROC, and the OA of the MSC for the physician with  
197 moderate to excellent reliability. For between operator ICC the following parameters: HE, hypodermis thickness, SWE  
198 skin, SWE hypodermis, SWE muscle, showed good to excellent reliability. The ICC for the OA and the skin thickness  
199 showed moderate to excellent reliability. For the inter-image analysis, within operator ICC showed excellent reliability  
200 for the hypodermis thickness parameter for both operators. The physician (operator 1) showed good to excellent

201 reliability for the ROC and HE. For the SWE skin parameter he showed moderate to excellent reliability; for the  
 202 opening angle parameter moderate to good reliability; for the remaining parameters poor to good reliability. The  
 203 engineer (operator 2) showed moderate to excellent reliability for the ROC, SWE skin, SWE hypodermis, and SWE  
 204 muscle parameters. For the opening angle parameter, the engineer showed moderate to good reliability; for the HE,  
 205 skin thickness poor to good reliability. The between operator ICC also showed excellent reliability for the hypodermis  
 206 thickness. The ICC for SWE skin parameter showed moderate to excellent reliability. The ICC of the remaining  
 207 parameters showed poor to good reliability.

208  
 209 *Table 2. Reliability assessment results with Intraclass correlation coefficient ICC for both intra-image and inter-image analysis*  
 210 *for both operators: 1 the physician and 2 the engineer.*  
 211

Parameter	Operator	Intra-image analysis		Inter-image analysis	
		Within operator ICC (95% CI)	Between operator ICC (95% CI)	Within operator ICC (95% CI)	Between operator ICC (95% CI)
Radius of curvature	1	0.86(0.68-0.94)	0.84(0.64-0.94)	0.90(0.79-0.96)	0.69(0.34-0.87)
	2	0.93(0.84-0.97)		0.76(0.53-0.90)	
Opening angle	1	0.86(0.66-0.94)	0.81(0.57-0.92)	0.74(0.53-0.89)	0.58(0.17-0.82)
	2	0.96(0.91-0.98)		0.73(0.50-0.88)	
Height	1	0.97(0.93-0.99)	0.97(0.92-0.99)	0.89(0.78-0.96)	0.74(0.43-0.89)
	2	0.98(0.95-0.99)		0.69(0.45-0.87)	
Skin thickness	1	0.94(0.87-0.97)	0.88(0.73-0.95)	0.71(0.49-0.87)	0.53(0.09-0.80)
	2	0.95(0.88-0.98)		0.59(0.32-0.80)	
Hypodermis thickness	1	0.99(0.99-1.00)	0.99(0.99-1.00)	0.98(0.96-0.99)	0.98(0.95-0.99)
	2	0.99(0.99-1.00)		0.99(0.98-1.00)	
SWE skin	1	0.99(0.99-1.00)	0.99(0.99-1.00)	0.83(0.67-0.93)	0.78(0.50-0.91)
	2	0.99(0.99-1.00)		0.85(0.72-0.94)	
SWE hypodermis	1	0.99(0.98-1.00)	0.98(0.94-0.99)	0.70(0.46-0.86)	0.65(0.27-0.85)
	2	0.98(0.97-0.99)		0.80(0.63-0.91)	
SWE muscle	1	0.96(0.88-0.99)	0.93(0.79-0.98)	0.71(0.41-0.90)	0.41(-0.22-0.80)
	2	0.98(0.96-1.00)		0.84(0.63-0.95)	

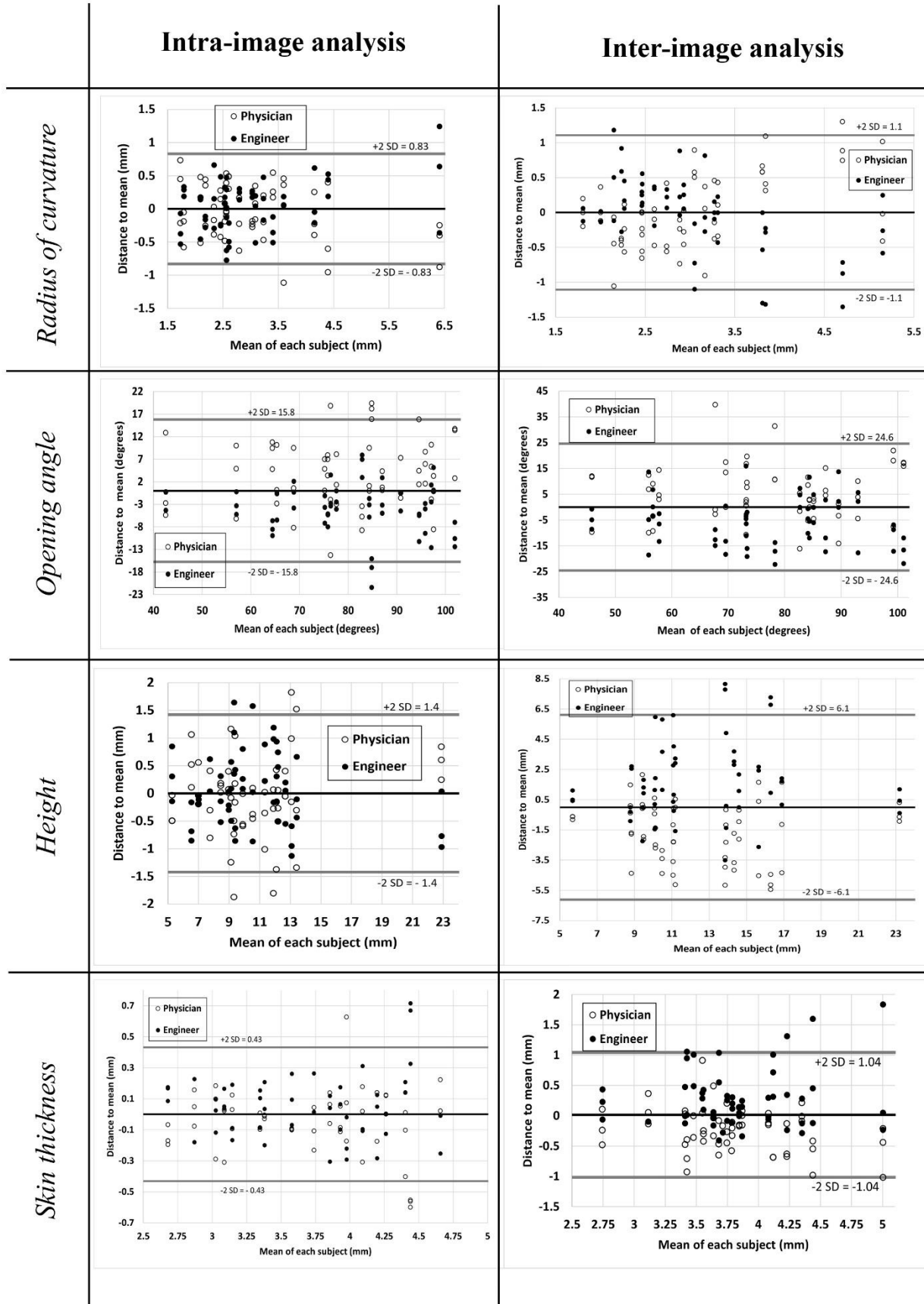
212

213

214  
215

216 *Agreement assessment*

217 The modified Bland Altman agreement plots for both the intra and inter image analysis are reported in figure 2. The  
218 95% limits of agreement with the mean varied from the intra to the inter-image analysis as follows: for the ROC from  
219  $\pm 0.83$  mm to  $\pm 1.1$  mm; for the opening angle from  $\pm 15.8$  degrees to  $\pm 24.8$  degrees; for the HE from  $\pm 1.4$  mm to  $\pm 6.1$   
220 mm; for the skin thickness from  $\pm 0.43$  mm to  $\pm 1.04$  mm; for the hypodermis thickness from 0.57 mm to 1.4 mm; for  
221 the SWE skin from  $\pm 0.03$  m/s to  $\pm 0.33$  m/s; for the SWE hypodermis from  $\pm 0.06$  m/s to  $\pm 0.29$  m/s; and for the SWE  
222 muscle from  $\pm 0.08$  m/s to  $\pm 0.25$  m/s.



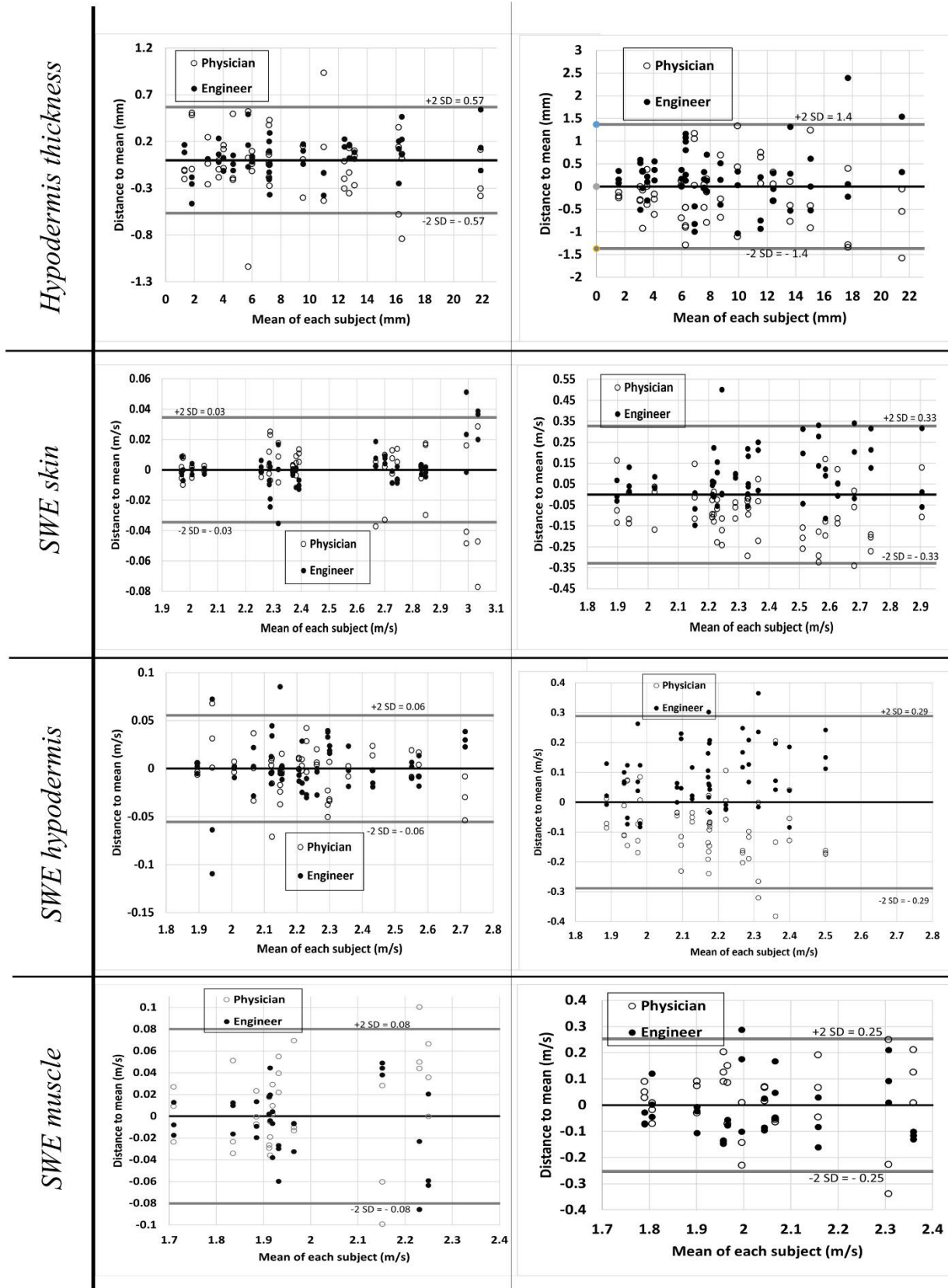


Fig. 2. Agreement plots with the mean of measurements for the intra-image and inter-image analyses for the 8 parameters

225 *Healthy Young adults VS healthy elderly*

226 The results of means, normality tests and Student’s t-test test are reported in table 3. There was insufficient evidence  
 227 to claim that the distributions were not normal or that the variances were not equal. Based on the results of the student  
 228 T-test, we concluded that there is a statistically significant difference only for the SWE of the muscle ( $2.11 \pm 0.27$  m/s  
 229 for the young adults group vs  $1.70 \pm 0.17$  m/s for the elderly, p-value = 0.001). Because of the relatively small sample  
 230 size, the sample means for each parameter were also compared with the Wilcoxon signed rank test. The conclusions  
 231 were the same i.e. there is a statistically significant difference only for the SWE of the muscle.

232 Images reported in figure 2 show observations for the older group subjects that diverged from the group. The upper  
 233 and lower limits for skin and hypodermis SWE were found in a 62-year-old male subject with a BMI of  $39.1 \text{ kg/m}^2$   
 234 (fig.2a) and a 67-year-old male with a BMI of  $27.4 \text{ kg/m}^2$  (fig.2b), respectively. A 62-year-old female elderly with a  
 235 BMI of  $22.3 \text{ kg/m}^2$  (fig.2c) showed a heterogeneous distribution of hypodermis thickness over the MSC.

236  
 237  
 238

Table 3. Mean of each parameter for the young adults group and healthy elderly, normality using Shapiro-wilk test and comparison using Student’s t-test.

Parameter		Young adults		Healthy elderly		Student’s t-test p-value
		Mean $\pm$ SD	Shapiro Wilk test p-value	Mean $\pm$ SD	Shapiro Wilk test p-value	
Bone anatomy (MSC)	OA (°)	80.32 $\pm$ 21.06	0.628	79.54 $\pm$ 19.19	0.509	0.920
	HE (mm)	10.39 $\pm$ 4.45	0.119	8.20 $\pm$ 2.94	0.293	0.159
	ROC (mm)	2.90 $\pm$ 1.21	0.191	2.19 $\pm$ 0.17	0.550	0.088
Tissue morphology	ST (mm)	3.61 $\pm$ 0.55	0.982	3.30 $\pm$ 0.53	0.215	0.147
	HT (mm)	8.67 $\pm$ 5.21	0.380	6.08 $\pm$ 3.56	0.457	0.156
Tissue stiffness	sSWE (m/s)	2.27 $\pm$ 0.28	0.087	2.22 $\pm$ 0.55	0.295	0.800
	hSWE (m/s)	2.06 $\pm$ 0.16	0.497	1.98 $\pm$ 0.33	0.437	0.465
	mSWE (m/s)	2.11 $\pm$ 0.27	0.128	1.70 $\pm$ 0.17	0.758	0.001

239



240

241

242

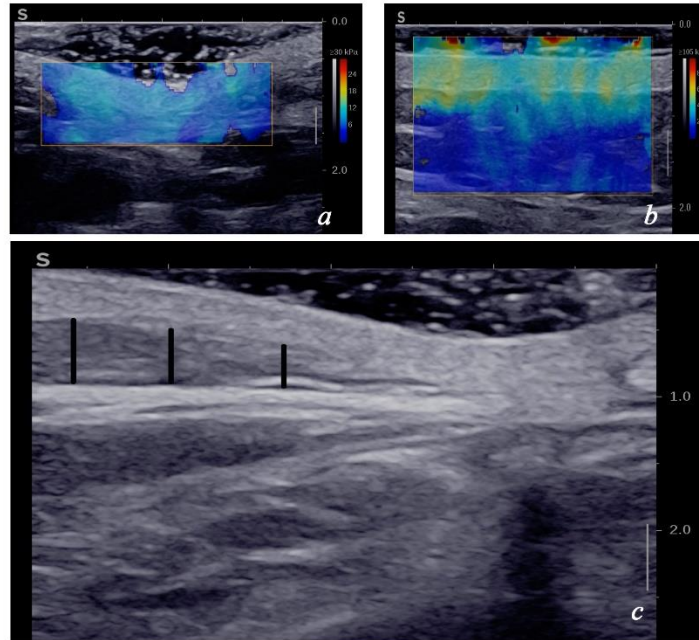


*Fig. 3. Observations in the elderly group: lowest and highest skin/hypodermis SWE signal (a,b respectively), hypodermis heterogeneous thickness distribution over the MSC (black vertical lines) (c)*

## 243 Discussion

244 This study aimed to evaluate the use of B-mode US and SWE in the assessment of bone geometry, tissue morphology  
245 and tissue stiffness in the context of sacral PU prevention in elderly. A protocol was developed to evaluate the region  
246 over the MSC. It was tested for reliability on a group of 19 healthy young subjects by two operators: a physician and  
247 an engineer. Afterwards, the protocol was tested on a group of 11 healthy older people by the physician only. The  
248 parameters evaluated by our protocol were: the radius of curvature (ROC), opening angle (OA), and height (HE) of  
249 the MSC for the bone geometry; the skin thickness (ST), and hypodermis thickness (HT) for the tissue morphology;  
250 skin shear wave velocity (sSWE), hypodermis shear wave velocity (hSWE), and muscle shear wave velocity (mSWE)  
251 for tissue stiffness.

### 252 1. Reliability study

253 The intra-image analysis was first conducted to assess the operators understanding and reliability of measuring each  
254 parameter. Within-operator ICC was good to excellent for all parameters for the engineer. For the physician, most  
255 parameters showed good to excellent reliability except for the ROC (CI 0.68-0.94) and OA (CI 0.66-0.94), showing  
256 moderate to excellent reliability. This might be due to an unclear definition of these two parameters. While the ROC  
257 is measured by placing points on the tip of MSC, the position of the start and ending points are not always clear.  
258 Between operator ICC, for the intra-image analysis, showed good to excellent reliability for all parameters except  
259 ROC, OA, ST with moderate to excellent reliability. These results also highlight the difficulty in choosing the points  
260 for the ROC and OA. For the ST parameter, although the skin is a continuous layer over the hypodermis, both stratum  
261 corneum : the most superficial layer of the epidermis, and the reticular layer: the lower part of the dermis, are wavy  
262 layers and thus might affect ST measurement depending on the part of the image chosen to assess ST [39]. The inter-  
263 image analysis aimed to test whether operators are capable of successfully repeating an acquisition three times and  
264 reproducing the acquisition protocol. Because acquisitions measured were not the same, ICC results were expected to  
265 have lower values. The discussion will involve only the parameters that showed good to excellent reliability on the  
266 intra-image analysis. First the HE parameter, within operator reliability was good to excellent for the physician but  
267 low to good for the engineer. A possible explanation might be that the acquisitions were not taken at the same level  
268 over the MSC. Another explanation is the fact that, in terms of anatomy, the sacrum is the most variable portion of the  
269 spine. In fact, the MSC is formed by the fusion of the spinous processes of the first three to four sacral vertebrae, and  
270 therefore bone morphology might differ from a level to another [40]. In this perspective, an emphasis should be on  
271 taking the acquisition at the level of the two PSIS, since it is a fixed, palpable and US visible anatomic landmark (using  
272 the curvilinear probe). Also, the only study, that the authors found in the literature, that included US and SWE tissue  
273 evaluation of the sacral region reported neither the protocol of measurement nor the US anatomic landmark used  
274 during acquisition [31]. The authors think that this biased the results since the anatomy of the sacrum is complex and  
275 irregular [40], [41].

276 For the shear wave velocity: within operator and between operator ICCs showed moderate to excellent reliability for  
277 the skin; low to good reliability for hypodermis and muscle for both within and between operator ICCs. Possible  
278 reasons include signal instability and inhomogeneity associated with tissue depth and operator's experience. Another  
279 reason might be tissue anisotropy, therefore tissue SWE signal depends on the orientation of the probe relative to the  
280 layer tested. Also, this affects much more muscular fibres since they're organised with a geometric alignment

281 compared with the less structured adipose tissue or skin [42]. This explains the larger gap observed in the CI of between  
282 operator ICC for the mSWE (table 2).

283 The agreement plots were drawn to assess clinical significance of difference between measurements even when a  
284 parameter showed good reliability [38]. In the absence of a gold standard imaging tool in our study the level of  
285 agreement necessary for confident usage remains uncertain. However, we hypothesized that the clinical difference  
286 between different groups is significantly higher than the uncertainty of the measurements. For the bone geometry  
287 parameters, previous studies focused on ischium morphology and its impact on internal soft tissue strain thus on the  
288 occurrence of PU using mainly FE models [23], [43]. Our aim was to combine the three bone parameters : ROC, OA,  
289 and HE to differentiate a sharp tip from a flat tip [44]. For our knowledge, no research was conducted on the impact  
290 of the shape of the MSC on surrounding tissue deformation. In fact, reliability of bone morphology assessment using  
291 ultrasound is controversial: [19] found good between operator reliability for ischial tuberosity (IT) radius of curvature  
292 but they only reported the average ICC = 0.712 , while [20] found poor reliability for estimating inferior curvature of  
293 the IT in both its short and long axis. The methodology for our protocol combining an intra-image and-inter image  
294 analysis seemed promising but, with lack of reliability in the results and no clinical baseline for the MSC morphology,  
295 no interpretation could be given to the agreement plots reported in figure 2 for these parameters.

296 For tissue morphology parameters, skin thickness showed low reliability and a 95% CI of agreement with the mean of  
297  $\pm 1.04$ mm for the inter-image analysis. With a maximum skin thickness reported in the literature of 4mm [39] this  
298 parameter needs further investigation before clinical use. A possible solution might be to tell operators to measure the  
299 ST directly over the MSC. In this perspective and since the linear probe is limited in depth and field of view, the first  
300 acquisition using the curvilinear probe is crucial for identifying and marking the level of the MSC, but also its exact  
301 position over the spine midline. In fact, previous studies investigating the inter-operator reliability of tissue thickness  
302 measurement over IT showed : excellent reliability for total thickness with an average ICC=0.948, also without  
303 reporting the confidence interval [19] ; moderate to excellent reliability (0.60-0.95) for skin and fat thickness [20].  
304 To our knowledge, no study investigated the reliability of measuring tissue thickness using US over the sacrum. On  
305 the other hand, hypodermis thickness parameter showed excellent reliability and a 95% CI of agreement with the mean  
306 of  $\pm 1.4$ mm for the inter-image analysis. Since hypodermis thickness is variable, and mainly related to body mass index  
307 [45] with a value exceeding sometimes 50mm over lumbar spine [46], the clinical significance of this agreement seems

308 plausible. However, the interpretation depends on another factor: the homogeneity of the distribution of the  
309 hypodermis over the sacrum. This is going to be discussed in the next section.

310 For tissue stiffness parameters, although reliability was not satisfactory for all three parameters: skin, hypodermis, and  
311 muscle; the 95% CI level of agreement with the mean of the inter-image analysis of  $\pm 0.33$  m/s;  $\pm 0.29$  m/s;  $\pm 0.25$  m/s  
312 respectively, was minimal. In fact, previous studies investigating changes of shear wave velocity values in specific  
313 circumstances or disease showed: with prolonged loading in elderly, shear wave velocity of superficial region (mainly  
314 skin + hypodermis) over IT varied from 2.5 m/s to 3.3 m/s [31]; contracture strips of the gluteal muscle showed a shear  
315 wave velocity of 7.23 m/s vs 1.84 m/s for a healthy muscle at the same position[47]. **Because** the aim of this evaluation  
316 is to point out subjects who significantly diverge from normal values, the SWE values for the three regions remain  
317 interesting to report. Nevertheless, interpretation should be taken with caution and further investigations are needed to  
318 increase reliability. Possible solutions might include operator's training, and taking SWE videos in the transverse and  
319 vertical directions, especially for muscle stiffness, since the properties parallel to the fibers are quite different from  
320 loading perpendicular to the fibers [48].

321

## 322 **2. Young adults vs healthy elderly**

323 The following discussion will highlight observations noted when comparing parameters of the young adults group and  
324 the healthy older people for the acquisitions conducted only by the physician. The interpretations cannot be generalized  
325 since reliability of measurements was not satisfactory.

326 For bone parameters, aging is associated with structural, geometric and bone volumetric density changes [49]. It is  
327 unclear how that might affect the external shape of the MSC; the similar median values in the boxplot, and the absence  
328 of statistical significance of differences between the means for the three parameters might suggest that there are no  
329 US changes observable. Therefore, the estimation of these parameters aims to evaluate the impact of bone geometry  
330 on tissue deformation independently from age difference.

331 For the tissue morphology parameters, the median values for both ST and HT were lower for the older group, but no  
332 statistical difference was noted between means. In fact, studies have shown that thinning of the skin, associated with  
333 age, is observed in subjects with more than 70 years [50] while our older age group had a mean age of  $65 \pm 2.4$  yrs.  
334 Nevertheless, the mean ST of the young adults group  $3.61 \pm 0.55$ mm was close to values previously reported for the  
335 skin over the sacrum like, for example, Yalcin et al [51] found a mean of  $3.2 \pm 0.5$ mm. Also studies comparing tissue

336 thickness differences between SCI patients without vs with history of PU showed total thickness average of 15.3 mm  
337 vs 9.5 mm over the apex of IT [25]. Thus, the difference is quantifiable, but the challenge remains to determine a risk  
338 threshold value at high-risk patients. On the other hand, an observation, not reported in the literature to our knowledge,  
339 was noted for the hypodermis thickness distribution over the sacrum. One subject (fig.2b) clearly showed thinning of  
340 HT from the lateral to medial spine. Possible causes might be a spinal deformation causing a shift in the hypodermis  
341 layer while the skin, loosely bonded to subjacent organs, can slide over and maintain the same thickness [39]. This  
342 highlights the importance of measuring the HT directly over the tip of the MSC instead of the thickest region as  
343 mentioned in our protocol. In fact, HT is considered as an important parameter affecting internal soft tissue response  
344 to load [23] and thus, PU risk.

345 For the tissue stiffness parameters, median shear wave velocity for skin, hypodermis, and muscle was lower for the  
346 elderly group. Only for the muscle the difference showed statistical significance ( $p=0.001$ ). In fact, physiologic aging  
347 is associated with a loss of muscle mass starting at the age of 30 [10]. This might be caused by the infiltration of fat  
348 tissue and connective tissue into skeletal muscle [52]. Previous studies suggest that this is associated with an increase  
349 in muscle stiffness [53] and, with continuous compression, a further increase in muscle stiffness leading to injury [54].

350 While our results seem contradictory, since we noted a decrease in shear wave velocity between the young and the  
351 elderly group, the signal was collected closer to the proximal attachment of the gluteus maximus (lateral to the sacro-  
352 coccygeal region) rather than the muscle belly. Moreover, most studies, evaluating tissue stiffness and PU, focused on  
353 the variation of stiffness with loading [31], [54], [55]. The complexity and duration of the exam, especially for high-  
354 risk subjects, makes it impossible to evaluate a large number in a loading position. That is why we proposed in our  
355 study to evaluate tissue characteristics in an off-loading position and determine normal ranges within homogenous  
356 groups. While studies suggest that aging is associated with a decline in skin stiffness [9], [56] making it more  
357 susceptible to PU, there is no specific threshold value proposed for increased risk. On the other hand, sustained  
358 pressure application was associated with an increase in tissue stiffness [31], [57], [58]. The two subjects presenting  
359 maximum and minimum skin/hypodermis baseline shear wave velocity in the elderly group (fig2.a; fig2.b) were  
360 overweight ( $BMI > 25 \text{ kg/m}^2$ ). It is known that BMI values have an impact on the biomechanical behavior of tissues  
361 [59], [60], further investigations are needed to evaluate changes in tissue elasticity associated with BMI changes. Also  
362 the mean values of sSWE and hSWE over the sacrum of the elderly group ( $2.22 \pm 0.55 \text{ m/s}$  and  $1.98 \pm 0.33 \text{ m/s}$

363 respectively) are close to values reported in the literature (2.5 m/s and 1.8 m/s respectively) for a similar sample of  
364 nine healthy volunteers with a mean age of  $70.1 \pm 4.8$  years [31].

365

### 366 3. Limits and perspectives

367 The lack of reliability of measures is the main limit of our study. This is mainly related to: difficulty in repeating  
368 acquisitions on the same anatomic level, definition of parameters, lack of signal stability, and ultrasound expertise.

369 Also, the patient's prone position might be problematic for higher risk subjects. The sample size and the number of  
370 operators is also a limitation of this study. However, the protocol we developed is clinically feasible and can be easily  
371 proposed to evaluate patients at bedside. The relatively easy palpation of the anatomic landmark (PSIS) allows the  
372 exam to be conducted by any physician or nurse. The perspectives include a review of the protocol to increase  
373 reliability and an evaluation of higher risk elderly in nursing homes. Also, this protocol can quantify all layers'  
374 characteristics including bone, muscle, hypodermis, and skin using only US and SWE. This might serve in - patient  
375 specific - finite element modeling since quantifying tissue strain and stress distribution over a bony prominence is  
376 essential in determining an injury threshold [23], [55], [61].

377

## 378 Conclusion

379 In this study, we developed a protocol using US and SWE to assess bone and tissue characteristics over the sacrum in  
380 the context of PU prevention in elderly. **It is the** first protocol that combines assessment of all layers over bony  
381 prominences using only one imaging technique.

382 The protocol's reliability was evaluated on a sample of young adults and then tested on a group of healthy older  
383 subjects. We provided a thorough description of anatomic landmarks on palpation and US visualization to ensure  
384 reproducibility and real clinical application. However, reliability was not satisfactory and further improvements of the  
385 protocol are needed. The results comparing the young to healthy older age group suggested that changes related only  
386 to age might affect tissue thickness and elasticity more than bone morphology, but this cannot be generalized or  
387 quantified before increasing reliability and sample size. On the other hand, an observation in one of the subjects of the  
388 elderly group was not found in the literature: a heterogeneous distribution of the hypodermis thickness over the

389 sacrum. In order to evaluate the use of this tool for PU risk assessment, it is essential to test it on a high-risk sample  
390 like elderly in nursing homes or long hospital stay.

391 Finally, our recommendations for the scientific community - when using US and SWE – are:

- 392 - anatomic palpation and US recognition using the curvilinear probe.
- 393 - report exact anatomic region and provide proof on the US image.
- 394 - when measuring thickness and SWE ensure that acquisition is taken pressure free directly over the bone  
395 prominence and not in the surrounding region.
- 396 - results cannot be generalized before testing for reliability.

397

## 398 **Acknowledgement**

399 This project has received funding from the European Union’s Horizon 2020 research and innovation program under  
400 the Marie Skłodowska-Curie grant agreement No. 811965.

401

## 402 **Conflict of interest**

403 None

404

## 405 **APPENDIX 1**

### 406 **Ultrasound and SWE protocol**

#### 407 *Position and anatomic landmarks*

408 The volunteer is asked to lie down in the prone position with a cushion under the pubis to reduce lumbar lordosis. The  
409 examiner inspects the skin to identify any redness/swelling over the sacral region. Then, he palpates the posterior  
410 superior iliac spine (PSIS) and recognizes the continuation of intergluteal cleft representing the midline of the spine.

411

412

413

414 *Curvilinear probe*

415 The curvilinear probe allows a large field of view and better visualization of deep layers. After applying gel on the  
416 skin or the probe, the examiner scans the sacral region between the two PSIS in B-mode transverse view. The MSC  
417 appears as a reverse V-shaped hyperechoic contour (fig.1a). Sliding the probe lateral to the midline allows the  
418 recognition of the round shaped PSIS (fig.1a). An image is captured showing the MSC and PSIS. The region is marked  
419 over the skin with a marker or medical tape.

420 NB: if PSIS is not visible on US the use of sagittal view of the sacrum allows to recognize the anatomic site of the  
421 MSC. The examiner can align the site in the middle of the US image and then rotate the probe 90 degrees to return to  
422 transverse view.

423 *Linear probe*

424 The linear probe is used to assess the superficial layers over the MSC. A thick layer of gel is applied directly on the  
425 midline of the marked level. The probe is then applied in the transverse B-mode view with minimum pressure.  
426 Artefacts from air bubbles appear as a linear hypoechoic signal perpendicular to skin layers. The examiner eliminates  
427 air bubbles using the probe or by adding and spreading the gel again. An image is captured showing the skin and  
428 adipose tissue, and the thick layer of gel over the skin (fig.1b).

429 The linear probe is also used in SWE mode at the same level with a thick gel layer and minimum pressure. The region  
430 of interest (ROI) covering the skin and adipose tissue is chosen, and the examiner waits for a homogeneous signal on  
431 the screen, increasing/decreasing elasticity range matching tissue stiffness. One measurement is three videos in SWE  
432 of 10 seconds each (or more if signal fluctuates). The last acquisition in SWE mode, for the gluteus maximus muscle,  
433 is taken lateral to the sacro-coccygeal region using the same procedure. The anatomic landmark is the sacral horns  
434 and sacro-coccygeal ligament described as the “frog sign”. The muscle fibers are described as horizontal echoic lines  
435 under the skin and hypodermis (fig1.c).

436

437

438

439



## 440 References

- 441 [1] NPIAP/EPUAP/PPPIA, *Prevention and Treatment of Pressure Ulcers/Injuries: Clinical practice Guideline. The*  
442 *International Guideline.*, Emily Haesler. Australia, 2019.
- 443 [2] Z. Moore and S. Cowman, "Pressure ulcer prevalence and prevention practices in care of the older person in the Republic  
444 of Ireland," *Journal of Clinical Nursing*, vol. 21, no. 3–4, pp. 362–371, 2012, doi: [https://doi.org/10.1111/j.1365-](https://doi.org/10.1111/j.1365-2702.2011.03749.x)  
445 [2702.2011.03749.x](https://doi.org/10.1111/j.1365-2702.2011.03749.x).
- 446 [3] T. E. Børsting, C. R. Tvedt, I. J. Skogestad, T. I. Granheim, C. L. Gay, and A. Lerdal, "Prevalence of pressure ulcer and  
447 associated risk factors in middle- and older-aged medical inpatients in Norway," *Journal of Clinical Nursing*, vol. 27, no.  
448 3–4, pp. e535–e543, Feb. 2018, doi: [10.1111/jocn.14088](https://doi.org/10.1111/jocn.14088).
- 449 [4] K. Agrawal and N. Chauhan, "Pressure ulcers: Back to the basics," *Indian J Plast Surg*, vol. 45, no. 2, pp. 244–254, 2012,  
450 doi: [10.4103/0970-0358.101287](https://doi.org/10.4103/0970-0358.101287).
- 451 [5] R. M. Allman, P. S. Goode, N. Burst, A. A. Bartolucci, and D. R. Thomas, "Pressure ulcers, hospital complications, and  
452 disease severity: impact on hospital costs and length of stay," *Adv Wound Care*, vol. 12, no. 1, pp. 22–30, Feb. 1999.
- 453 [6] M. Situm, M. Kolić, and S. Spoljar, "[QUALITY OF LIFE AND PSYCHOLOGICAL ASPECTS IN PATIENTS WITH  
454 CHRONIC LEG ULCER]," *Acta Med Croatica*, vol. 70, no. 1, pp. 61–63, Mar. 2016.
- 455 [7] Z. E. Moore and D. Patton, "Risk assessment tools for the prevention of pressure ulcers," *Cochrane Database Syst Rev*,  
456 vol. 2019, no. 1, Jan. 2019, doi: [10.1002/14651858.CD006471.pub4](https://doi.org/10.1002/14651858.CD006471.pub4).
- 457 [8] K. Balzer, C. Pohl, T. Dassen, and R. Halfens, "The Norton, Waterlow, Braden, and Care Dependency Scales: comparing  
458 their validity when identifying patients' pressure sore risk," *J Wound Ostomy Continence Nurs*, vol. 34, no. 4, pp. 389–  
459 398, Aug. 2007, doi: [10.1097/01.WON.0000281655.78696.00](https://doi.org/10.1097/01.WON.0000281655.78696.00).
- 460 [9] G. R. Boss and J. E. Seegmiller, "Age-Related Physiological Changes and Their Clinical Significance," *West J Med*, vol.  
461 135, no. 6, pp. 434–440, Dec. 1981.
- 462 [10] C. A. Harms, D. Cooper, and H. Tanaka, "Exercise physiology of normal development, sex differences, and aging,"  
463 *Compr Physiol*, vol. 1, no. 4, pp. 1649–1678, Oct. 2011, doi: [10.1002/cphy.c100065](https://doi.org/10.1002/cphy.c100065).
- 464 [11] A. L. Oliveira, Z. Moore, T. O Connor, and D. Patton, "Accuracy of ultrasound, thermography and subepidermal moisture  
465 in predicting pressure ulcers: a systematic review," *J Wound Care*, vol. 26, no. 5, pp. 199–215, May 2017, doi:  
466 [10.12968/jowc.2017.26.5.199](https://doi.org/10.12968/jowc.2017.26.5.199).
- 467 [12] S. Grubbs *et al.*, "The Effect of High Frequency Ultrasound on the Prevention of Pressure Ulcers in Long-term Care  
468 Patients," *The Internet Journal of Academic Physician Assistants*, vol. 7, no. 1, Dec. 2008, Accessed: Jul. 14, 2021.  
469 [Online]. Available: <https://ispub.com/IJAPA/7/1/11804>
- 470 [13] K. N. Scafide, M. C. Narayan, and L. Arundel, "Bedside Technologies to Enhance the Early Detection of Pressure  
471 Injuries: A Systematic Review," *Journal of Wound Ostomy & Continence Nursing*, vol. 47, no. 2, pp. 128–136, Apr. 2020,  
472 doi: [10.1097/WON.0000000000000626](https://doi.org/10.1097/WON.0000000000000626).
- 473 [14] C. w. j. Oomens, M. Broek, B. Hemmes, and D. l. Bader, "How does lateral tilting affect the internal strains in the sacral  
474 region of bed ridden patients? — A contribution to pressure ulcer prevention," *Clinical Biomechanics*, vol. 35, pp. 7–13,  
475 Jun. 2016, doi: [10.1016/j.clinbiomech.2016.03.009](https://doi.org/10.1016/j.clinbiomech.2016.03.009).
- 476 [15] A. Levy, K. Kopplin, and A. Gefen, "An air-cell-based cushion for pressure ulcer protection remarkably reduces tissue  
477 stresses in the seated buttocks with respect to foams: Finite element studies," *Journal of Tissue Viability*, vol. 23, no. 1, pp.  
478 13–23, Feb. 2014, doi: [10.1016/j.jtv.2013.12.005](https://doi.org/10.1016/j.jtv.2013.12.005).

- 479 [16] R. M. A. Al-Dirini, M. P. Reed, J. Hu, and D. Thewlis, "Development and Validation of a High Anatomical Fidelity FE  
480 Model for the Buttock and Thigh of a Seated Individual," *Ann Biomed Eng*, vol. 44, no. 9, pp. 2805–2816, Sep. 2016, doi:  
481 10.1007/s10439-016-1560-3.
- 482 [17] V. Luboz, M. Petrizelli, M. Bucki, B. Diot, N. Vuillerme, and Y. Payan, "Biomechanical modeling to prevent ischial  
483 pressure ulcers," *J Biomech*, vol. 47, no. 10, pp. 2231–2236, Jul. 2014, doi: 10.1016/j.jbiomech.2014.05.004.
- 484 [18] E. Linder-Ganz, N. Shabshin, Y. Itzchak, and A. Gefen, "Assessment of mechanical conditions in sub-dermal tissues  
485 during sitting: A combined experimental-MRI and finite element approach," *Journal of Biomechanics*, vol. 40, no. 7, pp.  
486 1443–1454, Jan. 2007, doi: 10.1016/j.jbiomech.2006.06.020.
- 487 [19] J. S. Akins *et al.*, "Feasibility of freehand ultrasound to measure anatomical features associated with deep tissue injury  
488 risk," *Med Eng Phys*, vol. 38, no. 9, pp. 839–844, Sep. 2016, doi: 10.1016/j.medengphy.2016.04.026.
- 489 [20] J. M. Swaine *et al.*, "Adaptation of a MR imaging protocol into a real-time clinical biometric ultrasound protocol for  
490 persons with spinal cord injury at risk for deep tissue injury: A reliability study," *Journal of Tissue Viability*, vol. 27, no.  
491 1, pp. 32–41, Feb. 2018, doi: 10.1016/j.jtv.2017.07.004.
- 492 [21] A. Macron, H. Pillet, J. Doridam, A. Verney, and P.-Y. Rohan, "Development and evaluation of a new methodology for  
493 the fast generation of patient-specific Finite Element models of the buttock for sitting-acquired deep tissue injury  
494 prevention," *Journal of Biomechanics*, vol. 79, pp. 173–180, Oct. 2018, doi: 10.1016/j.jbiomech.2018.08.001.
- 495 [22] J. Doridam, A. Macron, C. Vergari, A. Verney, P.-Y. Rohan, and H. Pillet, "Feasibility of sub-dermal soft tissue  
496 deformation assessment using B-mode ultrasound for pressure ulcer prevention," *J Tissue Viability*, vol. 27, no. 4, pp.  
497 238–243, Nov. 2018, doi: 10.1016/j.jtv.2018.08.002.
- 498 [23] A. Macron *et al.*, "Is a simplified Finite Element model of the gluteus region able to capture the mechanical response of  
499 the internal soft tissues under compression?," *Clinical Biomechanics*, vol. 71, pp. 92–100, Jan. 2020, doi:  
500 10.1016/j.clinbiomech.2019.10.005.
- 501 [24] S. Gabison, K. Hayes, K. E. Campbell, J. M. Swaine, and B. C. Craven, "Ultrasound imaging of tissue overlying the  
502 ischial tuberosity: Does patient position matter?," *Journal of Tissue Viability*, vol. 28, no. 4, pp. 179–185, Nov. 2019, doi:  
503 10.1016/j.jtv.2019.07.001.
- 504 [25] S. E. Sonenblum, D. Seol, S. H. Sprigle, and J. M. Cathcart, "Seated buttocks anatomy and its impact on biomechanical  
505 risk," *Journal of Tissue Viability*, Jan. 2020, doi: 10.1016/j.jtv.2020.01.004.
- 506 [26] Ł. Paluch, E. Nawrocka-Laskus, J. Wiczorek, B. Mruk, M. Frel, and J. Walecki, "Use of Ultrasound Elastography in the  
507 Assessment of the Musculoskeletal System," *Pol J Radiol*, vol. 81, pp. 240–246, May 2016, doi: 10.12659/PJR.896099.
- 508 [27] J. Bercoff, M. Tanter, and M. Fink, "Supersonic shear imaging: a new technique for soft tissue elasticity mapping," *IEEE*  
509 *Transactions on Ultrasonics, Ferroelectrics, and Frequency Control*, vol. 51, no. 4, pp. 396–409, Apr. 2004, doi:  
510 10.1109/TUFFC.2004.1295425.
- 511 [28] J.-F. Deprez, E. Brusseau, J. Fromageau, G. Cloutier, and O. Basset, "On the potential of ultrasound elastography for  
512 pressure ulcer early detection," *Medical Physics*, vol. 38, no. 4, pp. 1943–1950, 2011, doi: 10.1118/1.3560421.
- 513 [29] G. Dubois *et al.*, "Reliable protocol for shear wave elastography of lower limb muscles at rest and during passive  
514 stretching," *Ultrasound Med Biol*, vol. 41, no. 9, pp. 2284–2291, Sep. 2015, doi: 10.1016/j.ultrasmedbio.2015.04.020.
- 515 [30] R. M. S. Sigrist, J. Liau, A. E. Kaffas, M. C. Chammas, and J. K. Willmann, "Ultrasound Elastography: Review of  
516 Techniques and Clinical Applications," *Theranostics*, vol. 7, no. 5, pp. 1303–1329, 2017, doi: 10.7150/thno.18650.
- 517 [31] G. Schäfer, G. Dobos, L. Lünemann, U. Blume-Peytavi, T. Fischer, and J. Kottner, "Using ultrasound elastography to  
518 monitor human soft tissue behaviour during prolonged loading: A clinical explorative study," *Journal of Tissue Viability*,  
519 vol. 24, no. 4, pp. 165–172, Nov. 2015, doi: 10.1016/j.jtv.2015.06.001.

- 520 [32] R. Mansur, L. Peko, N. Shabshin, L. Cherbinski, Z. Neeman, and A. Gefen, "Ultrasound elastography reveals the relation  
521 between body posture and soft-tissue stiffness which is relevant to the etiology of sitting-acquired pressure ulcers,"  
522 *Physiol. Meas.*, vol. 41, no. 12, p. 124002, Jan. 2021, doi: 10.1088/1361-6579/abc66d.
- 523 [33] C. Vergari *et al.*, "Intervertebral disc characterization by shear wave elastography: An in vitro preliminary study," *Proc*  
524 *Inst Mech Eng H*, vol. 228, no. 6, pp. 607–615, Jun. 2014, doi: 10.1177/0954411914540279.
- 525 [34] K. McGraw and S. P. Wong, "Forming Inferences About Some Intraclass Correlation Coefficients," *Psychological*  
526 *Methods*, vol. 1, pp. 30–46, Mar. 1996, doi: 10.1037/1082-989X.1.1.30.
- 527 [35] M. A. Bujang, "A simplified guide to determination of sample size requirements for estimating the value of intraclass  
528 correlation coefficient: A review," *Archives of Orofacial Sciences*, vol. 12, pp. 1–11, Jun. 2017.
- 529 [36] J. J. Hebert, S. L. Koppenhaver, E. C. Parent, and J. M. Fritz, "A systematic review of the reliability of rehabilitative  
530 ultrasound imaging for the quantitative assessment of the abdominal and lumbar trunk muscles," *Spine (Phila Pa 1976)*,  
531 vol. 34, no. 23, pp. E848–856, Nov. 2009, doi: 10.1097/BRS.0b013e3181ae625c.
- 532 [37] T. K. Koo and M. Y. Li, "A Guideline of Selecting and Reporting Intraclass Correlation Coefficients for Reliability  
533 Research," *J Chiropr Med*, vol. 15, no. 2, pp. 155–163, Jun. 2016, doi: 10.1016/j.jcm.2016.02.012.
- 534 [38] M. Jones, A. Dobson, and S. O'Brian, "A graphical method for assessing agreement with the mean between multiple  
535 observers using continuous measures," *International Journal of Epidemiology*, vol. 40, no. 5, pp. 1308–1313, Oct. 2011,  
536 doi: 10.1093/ije/dyr109.
- 537 [39] "Skin. Mescher A.L.(Ed.)," in *Junqueira's Basic Histology Text and Atlas, 16e*, Book, Section vols., New York, NY:  
538 McGraw Hill, 2021. Accessed: May 17, 2021. [Online]. Available:  
539 [accessmedicine.mhmedical.com/content.aspx?aid=1180414032](https://accessmedicine.mhmedical.com/content.aspx?aid=1180414032)
- 540 [40] J. S. Cheng and J. K. Song, "Anatomy of the sacrum," *Neurosurgical Focus*, vol. 15, no. 2, pp. 1–4, Aug. 2003, doi:  
541 10.3171/foc.2003.15.2.3.
- 542 [41] M.-P. Baron-Sarrabère, A. Micheau, and C. Cyteval, "Sacrum, coccyx, articulations sacro-iliaques : technique  
543 radiologique et aspects normaux," [//www.em-premium.com/data/traites/rx/30-60680/](http://www.em-premium.com/data/traites/rx/30-60680/), Sep. 2016, Accessed: Dec. 27,  
544 2021. [Online]. Available: <https://ezproxy.usj.edu.lb:2170/article/1083162>
- 545 [42] M. Serafin-Król and A. Maliborski, "Diagnostic errors in musculoskeletal ultrasound imaging and how to avoid them," *J*  
546 *Ultrason*, vol. 17, no. 70, pp. 188–196, Sep. 2017, doi: 10.15557/JoU.2017.0028.
- 547 [43] A. Gefen, "Risk factors for a pressure-related deep tissue injury: a theoretical model," *Med Bio Eng Comput*, vol. 45, no.  
548 6, pp. 563–573, Jun. 2007, doi: 10.1007/s11517-007-0187-9.
- 549 [44] R. S. Candadai and N. P. Reddy, "Stress distribution in a physical buttock model: Effect of simulated bone geometry,"  
550 *Journal of Biomechanics*, vol. 25, no. 12, pp. 1403–1411, Dec. 1992, doi: 10.1016/0021-9290(92)90054-5.
- 551 [45] M. A. Gibney, C. H. Arce, K. J. Byron, and L. J. Hirsch, "Skin and subcutaneous adipose layer thickness in adults with  
552 diabetes at sites used for insulin injections: implications for needle length recommendations," *Current Medical Research*  
553 *and Opinion*, vol. 26, no. 6, pp. 1519–1530, Jun. 2010, doi: 10.1185/03007995.2010.481203.
- 554 [46] J. J. Lee *et al.*, "Fat Thickness as a Risk Factor for Infection in Lumbar Spine Surgery," *Orthopedics*, vol. 39, no. 6, pp.  
555 e1124–e1128, Nov. 2016, doi: 10.3928/01477447-20160819-05.
- 556 [47] R. Guo, X. Xiang, and L. Qiu, "Shear-wave elastography assessment of gluteal muscle contracture," *Medicine*  
557 *(Baltimore)*, vol. 97, no. 44, Nov. 2018, doi: 10.1097/MD.0000000000013071.
- 558 [48] P. Escobar, S. Wittles, S. Asfour, and L. Latta, "Mechanical Characteristics of Muscle, Skin and Fat - Elastic Moduli for  
559 Finite Element Modeling of Limbs," p. 4.

- 560 [49] B. L. Riggs *et al.*, “Population-Based Study of Age and Sex Differences in Bone Volumetric Density, Size, Geometry, and  
561 Structure at Different Skeletal Sites,” *Journal of Bone and Mineral Research*, vol. 19, no. 12, pp. 1945–1954, Dec. 2004,  
562 doi: 10.1359/jbmr.040916.
- 563 [50] C. Lasagni and S. Seidenari, “Echographic assessment of age-dependent variations of skin thickness,” *Skin Research and*  
564 *Technology*, vol. 1, no. 2, pp. 81–85, 1995, doi: 10.1111/j.1600-0846.1995.tb00022.x.
- 565 [51] E. Yalcin, M. Akyuz, B. Onder, H. Unalan, and I. Degirmenci, “Skin thickness on bony prominences measured by  
566 ultrasonography in patients with spinal cord injury,” *J Spinal Cord Med*, vol. 36, no. 3, pp. 225–230, May 2013, doi:  
567 10.1179/2045772312Y.0000000088.
- 568 [52] R. McCormick and A. Vasilaki, “Age-related changes in skeletal muscle: changes to life-style as a therapy,”  
569 *Biogerontology*, vol. 19, no. 6, pp. 519–536, 2018, doi: 10.1007/s10522-018-9775-3.
- 570 [53] H. Rahemi, N. Nigam, and J. M. Wakeling, “The effect of intramuscular fat on skeletal muscle mechanics: implications  
571 for the elderly and obese,” *J R Soc Interface*, vol. 12, no. 109, p. 20150365, Aug. 2015, doi: 10.1098/rsif.2015.0365.
- 572 [54] A. Gefen, N. Gefen, E. Linder-Ganz, and S. S. Margulies, “In Vivo Muscle Stiffening Under Bone Compression Promotes  
573 Deep Pressure Sores,” *Journal of Biomechanical Engineering*, vol. 127, no. 3, pp. 512–524, Jan. 2005, doi:  
574 10.1115/1.1894386.
- 575 [55] E. Linder-Ganz, N. Shabshin, Y. Itzchak, Z. Yizhar, I. Siev-Ner, and A. Gefen, “Strains and stresses in sub-dermal tissues  
576 of the buttocks are greater in paraplegics than in healthy during sitting,” *Journal of Biomechanics*, vol. 41, no. 3, pp. 567–  
577 580, 2008, doi: 10.1016/j.jbiomech.2007.10.011.
- 578 [56] S. Luebberding, N. Krueger, and M. Kerscher, “Mechanical properties of human skin in vivo: a comparative evaluation in  
579 300 men and women,” *Skin Research and Technology*, vol. 20, no. 2, pp. 127–135, May 2014, doi: 10.1111/srt.12094.
- 580 [57] A. Gefen, “The biomechanics of sitting-acquired pressure ulcers in patients with spinal cord injury or lesions,”  
581 *International Wound Journal*, vol. 4, no. 3, pp. 222–231, 2007, doi: 10.1111/j.1742-481X.2007.00330.x.
- 582 [58] N. Shoham and A. Gefen, “Deformations, mechanical strains and stresses across the different hierarchical scales in  
583 weight-bearing soft tissues,” *Journal of Tissue Viability*, vol. 21, no. 2, pp. 39–46, May 2012, doi:  
584 10.1016/j.jtv.2012.03.001.
- 585 [59] R. Sopher, J. Nixon, C. Gorecki, and A. Gefen, “Exposure to internal muscle tissue loads under the ischial tuberosities  
586 during sitting is elevated at abnormally high or low body mass indices,” *Journal of Biomechanics*, vol. 43, no. 2, pp. 280–  
587 286, Jan. 2010, doi: 10.1016/j.jbiomech.2009.08.021.
- 588 [60] J. J. Elsner and A. Gefen, “Is obesity a risk factor for deep tissue injury in patients with spinal cord injury?,” *Journal of*  
589 *Biomechanics*, vol. 41, no. 16, pp. 3322–3331, Dec. 2008, doi: 10.1016/j.jbiomech.2008.09.036.
- 590 [61] S. Loerakker *et al.*, “The effects of deformation, ischemia, and reperfusion on the development of muscle damage during  
591 prolonged loading,” *Journal of Applied Physiology*, vol. 111, no. 4, pp. 1168–1177, Jul. 2011, doi:  
592 10.1152/jappphysiol.00389.2011.

593

594

595

596

597

598

599

## List of figures

Figure 1	US acquisition protocol of the sacral region in the transverse view. In B-mode: the medial sacral crest (arrow) at the level of the PSIS (black triangle) (a), skin (arrow) and adipose tissue (white triangle) over MSC (b); in SWE mode: the skin and adipose tissue (c), gluteus maximus muscle (star) (d).
Figure 2	Agreement plots with the mean of measurements for the intra-image and inter-image analyses for the 8 parameters.
Figure 3	Observations in the older group: lowest and highest skin/hypodermis SWE signal (a,b respectively), hypodermis heterogeneous thickness distribution over the MSC (double arrow) (c).

600

601

## List of tables

Table 1	Description of parameter measurement post acquisition using a customized MATLAB algorithm
Table 2	Reliability assessment results with Intraclass correlation coefficient ICC for both intra-image and inter-image analysis for both operators: 1 the physician and 2 the engineer.
Table 3	Mean of each parameter for the young adults group and healthy elderly, normality using Shapiro-wilk test and comparison using Student's t-test

602